Inorg. Chem. **2009**, *48*, 4317−4330

Replacement of a Nitrogen by a Phosphorus Donor in Biomimetic Copper Complexes: a Surprising and Informative Case Study with Calix[6]arene-Based Cryptands

Diana Over,[†] Aurélien de la Lande,[‡,§,*] Xianshun Zeng,[†,⊥] Olivier Parisel,[‡] and Olivia Reinaud*[,†]

Laboratoire de Chimie et Biochimie Pharmacologiques et Toxicologiques, UMR CNRS 8601, Université Paris Descartes (Paris 5), 45 rue des Saints Pères, 75006 Paris, France, Laboratoire de Chimie Théorique, UMR CNRS 7616, Université Pierre et Marie Curie (Paris 6), 4, place Jussieu, F-75252, Paris Cedex 05, France, Key Laboratory of Display Materials & Photoelectrical Devices (Ministry of Education), School of Materials Science & Engineering, Tianjin University of Technology, Tianjin 300384, China, and Institute for Biocomplexity and Informatics, Department of Chemistry, University of Calgary, 2500 University Drive N.W., Calgary, Alberta, Canada T2N 1N4

Received November 23, 2008

The aim of the paper is to characterize Cu complexes in the $\boldsymbol{P^{Ar}N_3}$ environment provided by ligands derived from triphenylphosphine $P(C_6H_4CH_2NHR)_3$ and compare their coordination behavior and reactivity with those obtained with all-nitrogen ligands such as tren. It is shown that coordination of the PN_3 ligand (R = *i*Pr) to Cu(I) and Cu(II) leads to complexes whose coordination sphere is hardly controlled as they readily undergo decoordination of either one *N* or the *P* donor together with oxidation of the latter. In strong contrast, when grafted on the small rim of a calix[6]arene, the $\boldsymbol{P^{Ar}N_3}$ is geometrically constrained into a tripod that enforces the metal center to remain in the same environment with a P−Cu bond for both oxidation states. These calix[6]PN_3-based Cu(I) and Cu(II) complexes react readily with exogenous ligands, making a comparison with calix[6]tren-based copper complexes possible. Indeed, reactivity studies in solution highlight very different behaviors. The complex $[Cu(calix[6]PN_3)]^{2+}$ shows an unusual affinity for weak σ-donors (e.g., MeCN > EtOH), while the analogous cuprous complex, $[Cu(calix[6]PN_3)]^{+}$, displays a surprising affinity for hard *O*-donor ligands (EtOH, DMF), which has never been observed for the tren analogues. Even more surprising is the lack of reactivity of $[Cu(calix[6]PN_3)]^{+}$ toward dioxygen, which contrasts strongly with the high reactivity of the $[Cu(calix[6]tren)]^{+}$ complex. In an attempt to explain the observed differences in binding properties and reactivity, Density Functional Theory calculations and electronic spectra simulations were undertaken. They suggest that coordination of the soft $P(Ar)_3$ center allows to tune the metal ion properties, either by absorbing excess electron density from Cu(I), or by increasing the electronic density of Cu(II). This is due to the simultaneous presence of the phosphorus atom (σ-donor) in apical position and the aromatic groups (π-acceptors) bound to the P-atom.

Introduction

Copper is a ubiquitous metal that plays crucial roles in biology.[1−4] Copper enzymes, such as Peptidylglycine α-Hydroxylating Monooxygenase (PHM) or Dopamine β-Monooxygenase (DβH) are involved in neurotransmitter biosynthesis and hormone regulation.[5] These enzymes, catalyzing the insertion of an oxygen atom into a C−H bond, present two copper centers, Cu_H and Cu_M, separated by about 11 Å.[6] While the Cu_H site plays the role of an electron donor

* To whom correspondence should be addressed. E-mail: olivia.reinaud@parisdescartes.fr (O.R.), delaland@ucalgary.ca (A.d.l.L.).
† Université Paris Descartes.
‡ Université Pierre et Marie Curie.
§ University of Calgary.
⊥ Tianjin University of Technology.

(1) Kaim, W.; Rall, J. *Angew. Chem., Int. Ed.* **1996**, *35*, 43–60.
(2) Klinman, J. P. *Chem. Rev.* **1996**, *96*, 2541–2562.
(3) Solomon, E. I.; Chen, P.; Metz, M.; Lee, S.-K.; Palmer, A. E. *Angew. Chem., Int. Ed.* **2001**, *40*, 4570–4590.
(4) Bento, I.; Carrondo, M. A.; Lindley, P. F. *J. Biol. Inorg. Chem.* **2006**, *11*, 539–547.
(5) Klinman, J. P. *J. Biol. Chem.* **2006**, *281*, 3013–3016.
(6) Prigge, S. T.; Eipper, P. A.; Mains, R. E.; Amzal, L. M. *Science* **2004**, *304*, 864–867.

10.1021/ic802253t CCC: $40.75
Published on Web 04/17/2009

during the catalytic cycle and is coordinated to three histidine residues, Cu_M is the O_2-binding site and is coordinated to two histidine residues and one methionine residue. The exact role of this methionine residue has not yet been elucidated. However, it seems clear that its role in the catalytic mechanism is important.[7−9] Interestingly, recent studies concerning tyramine β-hydroxylase, a mono-oxygenase of the same family, revealed that the enzyme remains active when the methionine residue at the Cu_M site is mutated for a cysteine, whereas its replacement for a histidine suppresses the catalytic activity of the enzyme.[10] Indeed, this *S*-donor ligand must influence the reactivity of the Cu_M center as sulfur is a soft donor atom that better stabilizes the Cu(I) state than Cu(II), hence raising the associated redox potential.[11]

Most model compounds for the active site of Cu-enzymes present an all-nitrogen-based ligand, either tridentate or tetradentate.[12−17] They have allowed the characterization of $Cu(O_2)$ adducts side-on and end-on bound, respectively. Model studies using mixed N,S-donors are more scarce.[7,18−20] One major reason is the poor affinity of the Cu(II) state for a thioether donor because of its soft character associated to its neutral nature. Karlin and co-workers have published the first copper-O_2 adduct for such systems, an end-on peroxo complex in which the copper center still contains a thioether bond.[11] The design of model compounds that constrain the Cu(II) ion to remain in the close vicinity of a soft donor thus appears to be a key for studying its impact on the metal ion properties. In addition, the model compounds should also be able to preserve a labile coordination site on the metal center for substrate binding.

We are interested in the properties of copper ions constrained into a mononuclear environment to prepare suitable model compounds for mononuclear copper enzymes. Therefore, we have adopted a general strategy consisting of using supramolecular structures containing a nitrogenous coordination core and a hydrophobic pocket controlling the binding of exogenous ligands to the metal center.[21] As a hydrophobic pocket, the cone of a calix[6]arene is used, substituted at the small rim by amino ligands able to coordinate a transition metal ion.[22−30] Members of the last generation of these calix[6]arene-based ligands are calix[6]azacryptands, presenting three amino arms covalently linked to each other, thus covalently capping the calix[6]arene at the small rim. This creates a pocket for the copper ion held in place by a strong chelating effect,[31−35] while dimerization of the complex is precluded and any exogenous molecule can access the metal center exclusively through the hydrophobic channel of the calix[6]arene core.

In our system, the atom covalently linking the three nitrogenous arms is a donor itself. In the tren case, it is a nitrogen atom while in the $\boldsymbol{P^{Ar}N_3}$ case, it is a phosphorus atom (so-called calix[6]tren and calix[6]PN_3 ligands schematized in Figure 1). Their structure is quite similar as both provide a tripodal environment constrained by the calixmacrocycle with three secondary amines as equatorial donors. They differ, however, through the nature of the apical donor: either a nitrogen or a phosphorus atom. A comparison of their coordinating properties toward Cu(I) and Cu(II) appears to be of high interest as it would give valuable insights into the role of a soft donor (here *P*), compared to an intermediate one (*N*) on the reactivity of a mononuclear Cu center. Phosphine ligands are ubiquitous in organometallic and coordination chemistry but have never been employed as ligands for a biological model system simply because they are not found in proteins. Phosphines are generally good σ-donors but depending on the nature of their substituents, they can become quite strong π-acceptor ligands. The phosphine moiety grafted onto the small rim of the calix[6]arene cone is a triphenyl derivative (P^{Ar}). Hence,

(7) Lee, Y.; Karlin, K. D. Highlights of Copper Protein Active-Site Structure/Reactivity and Synthetic Model Studies. In *Concepts and Models in Bioinorganic Chemistry*; Metzler-Nolte, N., Kraatz, H.-B. Eds.; Wiley-VCH: New York, 2006; pp 363−395.
(8) (a) de la Lande, A.; Gérard, H.; Moliner, V.; Izzet, G.; Reinaud, O.; Parisel, O. *J. Biol. Inorg. Chem.* **2006**, *11*, 593–608. (b) de la Lande, A.; Parisel, O.; Gérard, H.; Moliner, V.; Reinaud, O. *Chem.—Eur. J.* **2008**, *14*, 6465–6473.
(9) Chen, P.; Solomon, E. I. *Proc. Nat. Acad. Sci., U.S.A.* **2004**, *101*, 13105–13110.
(10) Hess, C. R.; Wu, Z.; Ng, A.; Gray, E. E.; McGuirl, M. A.; Klinman, J. P. *J. Am. Chem. Soc.* **2008**, *130*, 11939–11944.
(11) Lee, D.-H.; Hatcher, L. Q.; Vance, M. A.; Sarangi, R.; Milligan, A. E.; Narducci Sarjeant, A. A.; Incarvito, C. D.; Rheingold, A. L.; Hodgson, K. O.; Hedman, B.; Solomon, E. I.; Karlin, K. D. *Inorg. Chem.* **2007**, *46*, 6056–6068; and references cited therein.
(12) Lewis, E. A.; Tolman, W. B. *Chem. Rev.* **2004**, *104*, 1047–1076.
(13) Mirica, L. M.; Ottenwaelder, X.; Stack, T. D. P. *Chem. Rev.* **2004**, *104*, 1013–1045.
(14) Itoh, S.; Fukuzumi, S. *Acc. Chem. Res.* **2007**, *40*, 592–600.
(15) Cramer, C. J.; Tolman, W. B. *Acc. Chem. Res.* **2007**, *40*, 601–608.
(16) Hatcher, L. Q.; Karlin, K. D. *J. Biol. Inorg. Chem.* **2004**, *9*, 669–683.
(17) Itoh, S. *Curr. Opin. Chem. Biol.* **2006**, *10*, 115–122.
(18) Aboelella, N. W.; Gherman, B. F.; Hill, L. M. R.; York, J. T.; Holm, N.; Young, V. G.; Cramer, C. J.; Tolman, W. B. *J. Am. Chem. Soc.* **2006**, *128*, 3445–3458.
(19) Zhou, L.; Powell, D.; Nicholas, K. M. *Inorg. Chem.* **2006**, *45*, 3840–3842.
(20) Kodera, M.; Kita, T.; Miura, I.; Nakayama, N.; Kawata, T.; Kano, K.; Hirota, S. *J. Am. Chem. Soc.* **2001**, *123*, 7715–7716.
(21) Reinaud, O.; Le Mest, Y.; Jabin I. In *Calixarenes Enter The Nanoworld*; Harrowfield, J., Vicens, J., Eds.; Springer: Dordrecht, Holland, 2006; Chapter 13.
(22) Blanchard, S.; Le Clainche, L.; Rager, M.-N.; Chansou, B.; Tuchagues, J. P.; Duprat, A.; Le Mest, Y.; Reinaud, O. *Angew. Chem., Int. Ed.* **1998**, *37*, 2732–2735.
(23) Rondelez, Y.; Rager, M.-N.; Duprat, A.; Reinaud, O. *J. Am. Chem. Soc.* **2002**, *124*, 1334–1340.
(24) Le Poul, N.; Campion, M.; Izzet, G.; Douziech, B.; Reinaud, O.; Le Mest, Y. *J. Am. Chem. Soc.* **2005**, *127*, 5280–5281.
(25) Rondelez, Y.; Sénèque, O.; Rager, M.-N.; Duprat, A. F.; Reinaud, O. *Chem.—Eur. J.* **2000**, *6*, 4218–4226.
(26) Rondelez, Y.; Bertho, G.; Reinaud, O. *Angew. Chem., Int. Ed.* **2002**, *41*, 1044–1046.
(27) Le Clainche, L.; Giorgi, M.; Reinaud, O. *Inorg. Chem.* **2000**, *39*, 3436–3437.
(28) Izzet, G.; Frapart, Y. M.; Prangé, T.; Provost, K.; Michalowicz, A.; Reinaud, O. *Inorg. Chem.* **2005**, *44*, 9743–9751.
(29) Izzet, G.; Akdas, H.; Hucher, N.; Giorgi, M.; Prangé, T.; Reinaud, O. *Inorg. Chem.* **2006**, *45*, 1069–1077.
(30) Le Poul, N.; Campion, M.; Douziech, B.; Rondelez, Y.; Le Clainche, L.; Reinaud, O.; Le Mest, Y. *J. Am. Chem. Soc.* **2007**, *129*, 8801–8810.
(31) Izzet, G.; Douziech, B.; Prangé, T.; Tomas, A.; Jabin, I.; Le Mest, Y.; Reinaud, O. *Proc. Natl. Acad. Sci. U.S.A.* **2005**, *102*, 6831–6836.
(32) Izzet, G.; Zeng, X.; Akdas, H.; Marrot, J.; Reinaud, O. *Chem. Commun.* **2007**, 810–812.
(33) Izzet, G.; Zeitouny, J.; Akdas-Killig, H.; Frapart, Y.; Ménage, S.; Douziech, B.; Jabin, I.; Le Mest, Y.; Reinaud, O. *J. Am. Chem. Soc.* **2008**, *130*, 9514–9523.
(34) Izzet, G.; Rager, M.-N.; Reinaud, O. *Dalton Trans.* **2007**, 771–780.
(35) Izzet, G.; Zeng, X.; Over, D.; Douziech, B.; Zeitouny, J.; Giorgi, M.; Jabin, I.; Le Mest, Y.; Reinaud, O. *Inorg. Chem.* **2007**, *46*, 375–377.

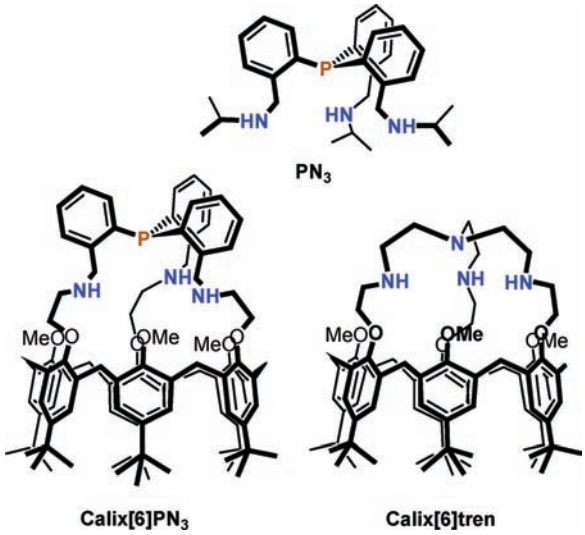

Figure 1. Schematic representation of the ligands considered herein.

when coordinated to a metal center, this ligand can behave as a donor as well as an acceptor.

So far, we had studied the coordination properties of tren-capped calix[6]arene ligands toward Cu(II) and Cu(I) as described recently.[31,33,34] For the $\boldsymbol{P^{Ar}N_3}$-capped calix[6]arene, a preliminary study related to the Cu(II) state has been reported.[35] It highlighted surprising properties of the calix[6]PN_3Cu(II) core compared to calix[6]trenCu(II). Here, we report a more complete study on Cu(I) and Cu(II) ions coordinated to two different $\boldsymbol{P^{Ar}N_3}$-cores, both of which present three secondary amino arms, however, with different geometrical constraints. In the first case, the *N*-donors are linked to relatively bulky iPr groups (the so-called "PN_3" ligand depicted in Figure 1), according to the "classical" design of model compounds. In the second case, the *N*-donors are geometrically constrained by the calix[6]arene macrocycle within the calix[6]PN_3 ligand. This allows to highlight the importance of the calix[6]arene cone for stability as well as for reactivity. We then compare the properties of Cu(I) and Cu(II) coordinated to calix[6]PN_3 with their tren analogues. Spectroscopic studies together with density functional theory (DFT) calculations will be presented and tentatively interpreted as the impact of *N*-donor substitution for a soft donor (*P*) on the Cu(I) and Cu(II) properties.

Results

Cu(I) and Cu(II) Coordination to PN_3. In strong contrast to the tren derivatives, ligands of $\boldsymbol{P^{Ar}N_3}$ type coordinated to copper centers have been only little explored in the literature. To our knowledge the reactivity of only one $\boldsymbol{P^{Ar}N_3}$-type ligand toward copper(I) and copper(II) ions has been reported by Lang and co-workers.[36−38] The ligand used, the *N*-dimethyl derivative of *tris*(2-aminomethyl)triphenylphosphine $P(C_6H_4CH_2NMe_2\text{-}2)_3$, is quite similar to the one reported here, except that the coordinating amino arms are composed of a tertiary amine. Several cuprous complexes have been reported, including some X-ray diffraction (XRD) structures, which illustrate that the coordination mode of this ligand depends on the counteranion present. Tetrahedral Cu(I) complexes were obtained, either in the $\boldsymbol{P^{Ar}N_3}$ environment provided by the tetradentate ligand or in the $\boldsymbol{P^{Ar}N_2X}$ environment in the presence of a coordinating anion X^- such as NO_3^- with one uncoordinated nitrogen arm. Complexation of Cu(II) with the same ligand has also been explored; however, no solution studies have been reported because of both their low solubility and their low stability, undergoing readily reduction to Cu(I). XRD structures have been obtained, however. They describe a Cu(II) center either in a $\boldsymbol{P^{Ar}N_3}$ *X* or in a $\boldsymbol{P^{Ar}N_2X}$ environment, thus further illustrating the easy removal of one nitrogen arm of the $P(C_6H_4CH_2\text{-}NMe_2\text{-}2)_3$ ligand from the coordination sphere of the metal ion.

The *N*-isopropyl derivative of the *tris*(2-aminomethyl)-triphenylphosphine core, ligand PN_3, was synthesized within two steps from *tris*(2-carboxaldehyde)triphenylphosphine, by means of a condensation-reduction sequence with isopropylamine.[39] The corresponding cuprous complex was prepared with equivalent amounts of ligand and $[Cu(MeCN)_4]PF_6$ in a 1:1 mixture of acetonitrile and dichloromethane giving a pale yellow solid. The ^{31}P NMR at room temperature (RT) in CD_3CN gave, besides a very sharp septuplet at 61.32 ppm for the PF_6 counterion, a very large resonance (1515 Hz) at −37 ppm for the cuprous cation, consistent with the coordination to the phosphorus atom.[40−44] The ^1H NMR spectrum of the complex showed a C_{3v} symmetry signature at 300 K. When comparing the spectrum of the cuprous complex with that of the free ligand, spectral changes attested to a modification of their chemical environment upon coordination of the amino arms to the metal center: the isopropyl protons were shifted upfield (0.2 ppm for the methyl groups and 0.3 ppm for CH) whereas the aromatic protons were shifted downfield (0.1 to 0.2 ppm). When lowering the temperature, the methylene resonances started to split and the methyl peaks to broaden (270 K), while at 230 K the spectrum displayed some disymmetrical pattern. As complexes with comparable $\boldsymbol{P^{Ar}N_3}$ ligands have been shown to crystallize mainly in a tetrahedral geometry, such dynamic features might be explained by the coordination/decoordination of one amino arm from the metal center, a process that is fast on the NMR time scale at RT. All this

(36) Leschke, M.; Lang, H.; Melter, M.; Rheinwald, G.; Weber, C.; Mayer, H. A.; Pritzkow, H.; Zsolnai, L.; Driess, A.; Huttner, G. *Z. Anorg. Allg. Chem.* **2002**, *628*, 349–356.
(37) Leschke, M.; Melter, M.; Walfort, B.; Driess, A.; Huttner, G.; Lang, H. Z. *Anorg. Allg. Chem.* **2004**, *630*, 2022–2030.
(38) Lang, H.; Shen, Y.; Rüffer, T.; Walfort, B. *Inorg. Chim. Acta* **2008**, *361*, 95–102.
(39) Whitnall, M. R.; Hii, K. K.; Thornton-Pett, M.; Kee, T. P. *J. Organomet. Chem.* **1997**, *529*, 35–50.
(40) Broad resonances in the ^{31}P NMR spectra of cuprous phosphine complexes are generally observed because of quadrupolar interactions involving the copper metal center ($I_{Cu} = 3/2$) and to fluxional behavior in solution. See refs 41−44.
(41) Szlyk, E.; Kucharek, R.; Szymanska, I. *J. Coord. Chem.* **2001**, *53*, 55–67.
(42) Comba, P.; Katsichtis, C.; Nuber, B.; Pritzkow, H. *Eur. J. Inorg. Chem.* **1999**, 777–783.
(43) Berners-Price, S. J.; Johnson, R. K.; Mirabelli, C. K.; Faucette, L. F.; McCabe, F. L.; Sadler, P. J. *Inorg. Chem.* **1987**, *26*, 3383–3387.
(44) Garcia-Seijo, M. I.; Sevillano, P.; Gould, R. O.; Fernandez-Anca, D.; Garcia-Fernandez, M. E. *Inorg. Chim. Acta* **2003**, *353*, 206–216.

accounts for the probable formation of a tetrahedral Cu(I) complex that, in MeCN solution, undergoes exchanges of its amino-arms because of the coordination of one solvent molecule as a fourth donor. Such a behavior is further supported by DFT calculations (vide infra). In the non-coordinating solvent $CDCl_3$, the complex is less soluble; however, a spectrum could be obtained showing only broad resonances, suggesting an ill-defined environment for the metal ion. Bubbling CO into a solution of $[Cu(I)PN_3]^+$ in CH_2Cl_2 led to the formation of a Cu(I)-CO adduct as evidenced by an intense IR stretch at $\nu_{CO} = 2081$ cm^{-1}.

Complex $[Cu(I)PN_3]^+$ is unstable in air in the solid state, undergoing fast autoxidation to give a number of unidentified copper(II) compounds. When O_2 was bubbled into a CH_2Cl_2 solution of complex $[Cu(I)PN_3]^+$, the solution turned green very rapidly, even at −78 °C, and electron paramagnetic resonance (EPR) spectroscopy confirmed the formation of several Cu(II) compounds, all with a tetragonal geometry but without superhyperfine coupling to the phosphorus atom. ESI mass analysis of the products showed a peak at m/z = 492.5 corresponding to ($O{=}PN_3 + H^+$), thus indicating phosphine oxidation. In MeCN, however, the yellow complex $[Cu(I)PN_3]^+$ remained stable vs O_2 for hours, which shows that bound acetonitrile efficiently protects the metal center from auto-oxidation.

When reacting equimolar amounts of the PN_3 ligand with $[Cu(H_2O)_6](ClO_4)_2$ in a non-coordinating solvent such as tetrahydrofuran (THF), the syntheses invariably led to a mixture of Cu(II) complexes that evolved in solution depending on the concentration and the basicity of the medium (additional Et_3N). Only when carried out under neutral conditions in a 1:1 mixture of acetonitrile and dichloromethane, the procedure allowed the isolation of a single compound that crystallized out of the solution. The resulting green solid Cu(II) complex revealed to be air sensitive and completely insoluble in almost all common solvents, coordinating or not (CH_2Cl_2, THF, $CHCl_3$, MeCN), except DMF in which decoordination occurred (releasing free Cu(II) as detected by EPR). In presence of dioxygen, or simply in air, bleaching occurred (within hours), thus indicating reduction of Cu(II) to Cu(I) with concomitant phosphine oxidation to $O{=}PN_3$ as shown by ESI mass analysis. One way to characterize the green cupric complex was by solid state EPR spectroscopy (Figure 2). Simulation of the spectrum gave good results with three g values, two of which are very close ($g_1 \approx g_2 < g_3$), thus indicating a $d_{x^2-y^2}$ ground state with an only slightly distorted axial geometry. The strong anisotropic superhyperfine coupling with the phosphorus atom on the perpendicular components attests to its coordination to the Cu(II) center. On the basis of this information a square pyramidal geometry is proposed for this $Cu(II)PN_3$ complex, where the P-atom, two amino arms, and most probably an acetonitrile molecule (reminiscent from the synthesis) represent the base of the pyramid, while the third amino arm is in an axial position. Because of the insolubility of this compound and its air sensitivity no further studies were carried out.

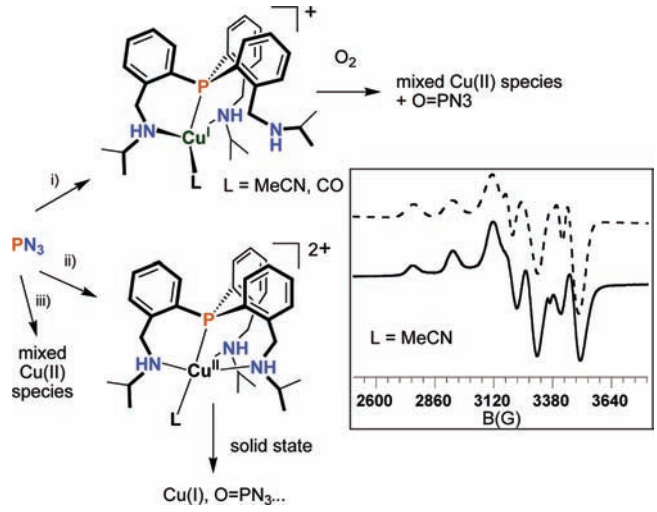

Figure 2. General scheme for the complexation of Cu to PN_3. (i) $Cu(MeCN)_4PF_6$ in CH_2Cl_2/MeCN; L = MeCN in MeCN, L = CO in CH_2Cl_2 under a CO atmosphere. (ii) $Cu(H_2O)_6(ClO_4)_2$ in CH_2Cl_2/MeCN or (iii) in THF. Inset: experimental (bottom) and simulated (top) EPR spectra of the isolated cupric complex based on ligand PN_3 (solid state, X-band, 100 K). $g_1 = 2.010$ ($A_1^P = 195$, $A_1^{Cu} = 27 \times 10^{-4}$ cm^{-1}); $g_2 = 2.050$ ($A_2^P = 228$, $A_2^{Cu} = 30$ x10^{-4} cm^{-1}); $g_3 = 2.220$ ($A_3^P = 20$, $A_3^{Cu} = 172 \times 10^{-4}$ cm^{-1}).

All in all, this first study, summarized in Figure 2, confirms that PN_3 is a potential ligand for copper in both oxidation states. The cuprous complex, most likely in a tetrahedral geometry, binds π-acceptors such as a nitrile or CO. It also shows a high reactivity toward O_2 in the solid state and in non-coordinating solvents. The corresponding cupric complex, prepared and isolated from MeCN, exhibits poor solubility and stability in solution. As for the auto-oxidation products, the P−Cu bond is readily lost in solution, allowing the Cu(II) complex to undergo uncontrolled rearrangements and ligand decoordination together with phosphine oxidation.

Cu(II) Coordination to Calix[6]PN$_3$. Coordination of cupric ions by the calixarene-based ***P^{Ar}N$_3$*** system was recently described.[35] Cu(II) complexes $[Cu(calix[6]PN_3)(L)]^{2+}$ were readily obtained upon stoichiometric reaction of copper(II) perchlorate with the ligand. The aqua complex (guest ligand L = H_2O) was isolated from THF as an air-stable blue-green complex. In strong contrast to the above-described $PN_3Cu(II)$ complex, this complex was very stable in solution as well, and no phosphine oxidation has been observed, which allowed the study of its host−guest behavior. The water ligand was easily substituted for a variety of guests such as nitriles, amides, and alcohols. XRD analysis (Figure 3, left) of the DMF adduct, $[Cu(calix[6]PN_3)(DMF)]^{2+}$, showed a 5-coordinate Cu(II) center with all donors of the ***P^{Ar}N$_3$*** cap strongly bound and the DMF ligand situated in the heart of the calixarene cavity. Solution EPR spectra (Figure 3, right) showed the maintainance of the P−Cu(II) bond ($A^P \cong 116-230 \times 10^{-4}$ cm^{-1}) and a trigonal bipyramidal (TBP) geometry for all guests ($g_1 \approx g_2 > g_3$). This was also confirmed by UV−vis absorption as, in each case (L = DMF, MeCN, EtOH, H_2O), the spectrum presented three d-d transitions between 550 and 850 nm that are characteristic of a more or less distorted TBP geometry.[31,32,35] It also showed one intense band at about 400

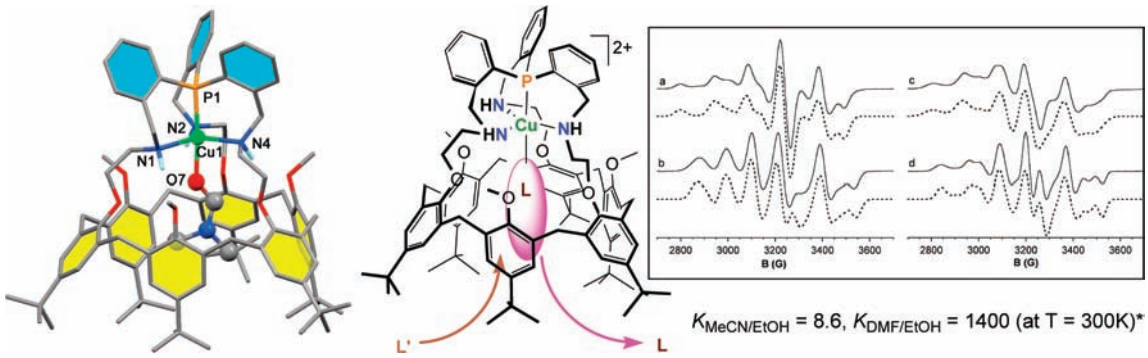

Figure 3. XRD[35] (left) with L = DMF and schematic representation of the $[Cu(calix[6]PN_3)(L)]^{2+}$ complexes. Selected bonds length [Å] and angles [deg]: Cu–O 2.02, Cu–N_{av}. 2.10, Cu–P 2.26, O–Cu–N_{av} 87.1, O–Cu–P 175.5, N–Cu–N_{av} 119.7 N–Cu–P_{av} 93.0. *: see ref 45. Inset: EPR spectra (X band) of $[Cu(calix[6]PN_3)(L)](ClO_4)_2$ in frozen dichloromethane (100 K) before ((a) L ≅ H_2O) and after addition of guest L (10% v/v): (b) L ≅ MeCN, (c) L ≅ EtOH, (d) L ≅ DMF.

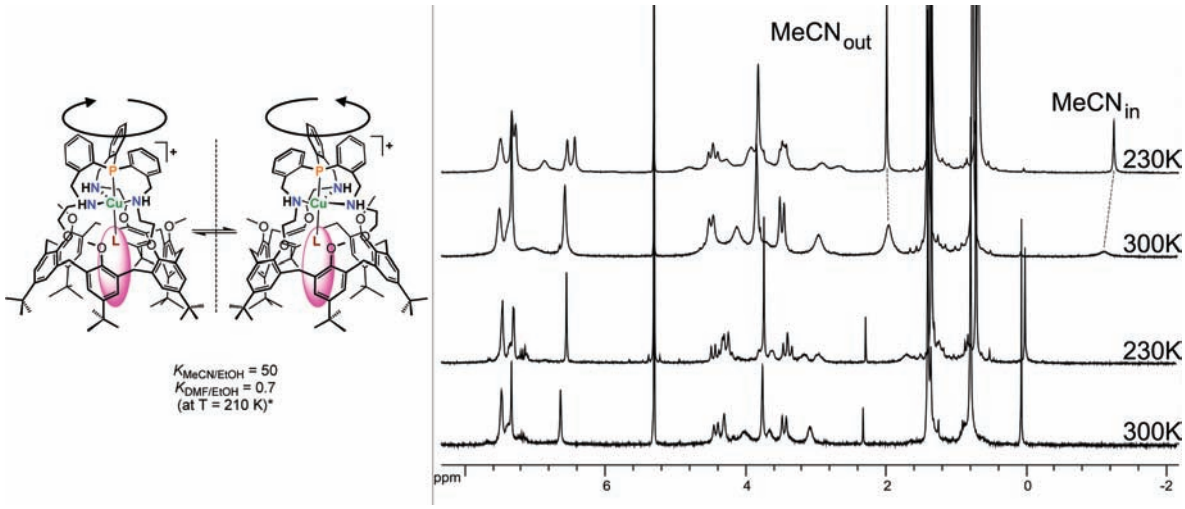

Figure 4. Right: ^{1}H NMR spectra (CD_2Cl_2, 250 MHz) of $[Cu(calixPN_3)(MeCN)]PF_6$ in the presence of 3 equiv of CH_3CN (top) and $[Cu(calixPN_3)]OTf$ in the presence of 1 equiv of toluene (bottom) at 300 and 230 K. Left: schematic representation of the cuprous complexes with a guest ligand L. *: see ref 45.

nm (ε = 1400−2000 M^{-1} cm^{-1}), the origin of which was obscure. Its invariability toward the nature of the coordinated guest (same energy and intensity with π-donors or π-acceptors) suggested that this transition corresponds to a charge transfer between the ***P^{Ar}N$_3$*** core and the Cu(II) center (vide infra).

Competition experiments gave the following order of relative affinities of Cu(II) for L: EtOH (1) < MeCN (8.6) ≪ DMF (1400). The affinity of MeCN was surprisingly higher than that of EtOH, and DMF displayed an unusually high affinity for the calix[6]PN_3 complex in comparison to the other poly(aza)-based complexes. A careful comparison of the present XRD structure with those reported for related calix[6]-based complexes hosting DMF did not provide any evidence of any significant difference in the positioning of the DMF guest in the calix-cone. Thus, the exceptional affinity of the metal center for DMF does not seem to be due to some steric effects but rather to stem from the different electronic properties of the Cu(II) center because of the phosphorus ligand in the apical position. This aspect has been investigated by means of quantum chemistry calculations that will be presented in the last part of this article.

Cu(I) Coordination to Calix[6]PN_3. Two different cuprous complexes were synthesized and isolated with the calix[6]PN_3 ligand. The first one was prepared starting from equimolar amounts of ligand and $[Cu(MeCN)_4]PF_6$ in a 1:1 mixture of acetonitrile and dichloromethane giving a pale yellow solid that was identified as $[Cu(calix[6]PN_3)(MeCN)]PF_6$. The complex $[Cu(I)(calix[6]PN_3)]OTf$ containing no coordinated organic guest ligand in the cavity was obtained by reacting equimolar amounts of ligand and $[Cu(toluene)_{1/2}]OTf$ in toluene.

$[Cu(calix[6]PN_3)(MeCN)]PF_6$. When isolated as a solid but not strongly dried compound, the hexafluorophosphate cuprous complex contained about 3 molar equiv of acetonitrile because of its synthesis. Its ^{1}H NMR spectrum at RT in CD_2Cl_2 showed a compound with a C_{3v} symmetry (Figure 4, top). A peak at −1.15 ppm showed the coordination of one molecule of acetonitrile ($MeCN_{in}$) to the cuprous center that is in slow exchange with free acetonitrile ($MeCN_{out}$). Its upfield shifted value attests to its inclusion into the heart of the aromatic core of the calix[6]arene. The downfield shift of the methoxy peak (4.01 ppm) compared to the free ligand

(45) The relative affinity of the Cu center for a guest L′ vs another guest L is defined by the following equilibrium constant: $K_{L'/L}$: Cu−L + L′ ⇆ Cu−L′ + L.

(2.88 ppm in $CDCl_3$) indicates that they are expelled out of the calixarene cone because of the inclusion of the MeCN guest. As a consequence, the calixarene macrocycle adopts a flattened cone conformation with three *t*Bu substituents in *out* position (1.40 ppm), while the three others are *in* (0.76 ppm), thus closing the cavity entrance. When lowering the temperature to 210 K, the $MeCN_{in}$ and $MeCN_{out}$ resonances sharpened, indicating the slowing down of the exchange process. The resonances due to the aromatic and methylenic protons split, while no change was observed for the OMe and *t*Bu groups. Such a behavior, well-known for this calix[6]arene-based type of metal complexes,[21,25,26] is due to the helical wrapping of the aza arms that are bound to the metal center. For these compounds, a conformational equilibrium between two enantiomeric forms (Figure 4, left), fast on the NMR time scale at RT, is slowed down at low temperature, thus allowing the distinction of the diastereotopic protons because of the helical structure induced by the $P^{Ar}N_3$ cap.

The ^{31}P NMR spectrum of the complex in CD_2Cl_2 revealed a sharp septuplet at −61.3 ppm for the PF_6^- anion and a broad (304 Hz) singlet at −46.0 ppm attributed to the $[Cu(calix[6]PN_3)(MeCN)]^+$ complex. The latter value is significantly upfield shifted compared to the free ligand (−34.7 ppm in $CDCl_3$), thus accounting for the coordination of the phosphorus atom to the metal center.

[Cu(calix[6]PN$_3$)]OTf. When directly isolated from a toluene solution, the triflate cuprous complex contained 1 molar equiv of toluene. Its ^1H NMR spectrum (Figure 4, bottom) in CD_2Cl_2 at RT showed a C_{3v} symmetry signature for the ligand, similar to that observed for the nitrilo PF_6 complex, besides free toluene. The methoxy groups, displaying a resonance at 3.75 ppm, are less expelled from the calixarene core than in the above-described nitrilo complex. At 210 K, splitting of the diastereotopic methylene protons was also observed, although almost no change was detected for the aromatic calixarene walls, besides a small upfield shift for the calix-aromatic protons located in an *in*-position (from 6.63 to 6.52 ppm), which is indicative of a slight flattening of the calix cone. Hence, in the absence of a guest ligand in the cavity the helical chirality, which is initiated by the coordination of Cu(I) to the $P^{Ar}N_3$ cap, is not efficiently transmitted to the host macrocyclic structure as it is when the latter is filled with the organic guest MeCN. The Cu(I)-phosphorus bond was characterized by a single, relatively broad (793 Hz) ^{31}P resonance at −70 ppm in CD_2Cl_2. This value is significantly upfield shifted compared to the nitrilo adduct (−46.0 ppm), thus accounting for the coordination of the phosphorus atom to a more electron-rich metal center.

Guest Binding. When adding a stoichiometric quantity of MeCN to the triflate cuprous complex, a ^1H resonance at −1.15 ppm appeared, attesting to its coordination to Cu(I) at RT, as above-described with the PF_6 complex. This shows the high affinity of the cuprous center for a small nitrilo guest.[46] In contrast, when *O*-donor ligands such as DMF or EtOH were added to a CD_2Cl_2 solution of the free triflate complex, the RT spectra did not show any upfield resonances that would be indicative of their endo-coordination. This, at first sight, was not surprising in view of the well-known poor affinity of soft metal centers for hard donors and indeed, their coordination has never been observed in any of our calixarene-based Cu(I) complexes with a poly(aza) environment. Quite surprisingly however, when the solution of [Cu(I)(calix[6]PN_3)]OTf containing 15 mol equiv of DMF was cooled down to 210 K, two new peaks, detected at −0.25 and −0.4 ppm, showed DMF *endo*-coordination. Integration of these resonances indicated that, under these conditions, about 20% of the Cu(I) centers bound DMF. Upon subsequent addition of 15 equiv of EtOH to the same solution, the upfield shifted DMF resonances vanished in favor of a triplet at −1.74 ppm because of the methyl group of ethanol in the cavity. Saturation transfer experiments confirmed these attributions, and integration of the spectra allowed to estimate the affinity constant $K_{DMF/EtOH} = 0.7$. A similar competition experiment carried out at the same *T* (210 K) with EtOH and MeCN gave $K_{MeCN/EtOH}$ estimated to 50. Even though the spectra became relatively complicated under these conditions (two different species, freezing of the helical conformation at low temperature), the two singlets of the *t*Bu-groups barely changed, which corroborates the fact that the system kept its C_3 axis for these three organic guest ligands.

Bubbling CO into a solution of the cuprous complex in CD_2Cl_2 containing ethanol, but no acetonitrile, changed dramatically the 210 K ^1H NMR spectrum. The triplet for the methyl group of $EtOH_{in}$ disappeared, indicating that ethanol was chased from the cavity and replaced by CO. The corresponding low temperature NMR signature of the calixarene host showed a complete loss of symmetry (Figure 5) with five different resonances for its *t*Bu substituents. One of them is particularly upfield shifted (from 0.78 to 0.49 ppm), which is indicative for self-inclusion of one *t*Bu group as has been described for other related Cu(I)CO complexes with calix[6]arene-based ligands.[25,26,34] The coordination of CO to the cuprous ion was further confirmed by IR spectroscopy. The solution spectrum of the calixarene-based complex (RT, 10 mM for Cu(I) in CD_2Cl_2 saturated with CO) showed a single ν_{CO} band at 2085 cm^{-1}, a value close to the one observed for the PN_3 complex.

Finally, in strong contrast to the $[Cu(I)PN_3]^+$ complex, the Cu(I) center bound to the calix[6]PN_3 ligand did not exhibit any reactivity toward O_2. When bubbling O_2 into solutions of the complex dissolved in a variety of solvents (CH_2Cl_2, THF, EtOH, toluene, MeCN), no visual change occurred over a period of 3 weeks, and EPR analyses showed only a very weak signal for Cu(II). The inertness toward dioxygen was also verified by ^1H NMR analyses in CD_2Cl_2 saturated with O_2 over a period of 5 days. Analyses by mass

(46) Surprisingly, the nitrilo cuprous complex appeared to be sensitive to the presence of water. Indeed, addition of about 20 mol equiv of H_2O led to the vanishing of the $MeCN_{in}$ peak associated to some broadening of the calixarene resonances, without δ-shift, however. This suggests that the presence of H_2O labilizes the nitrilo−guest, a phenomenon that has *not* been observed with the poly(aza)-based calixarene cuprous complexes studied so far.

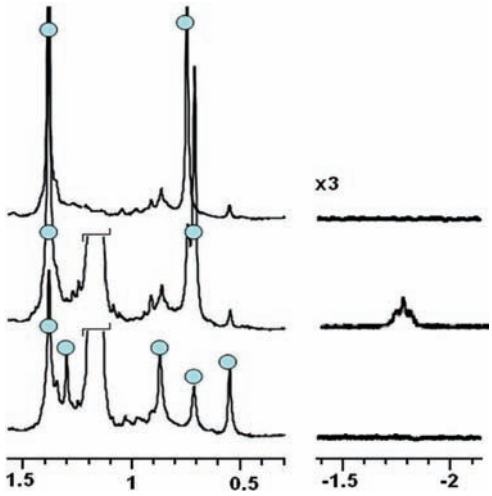

Figure 5. Selected high-field areas of the ^{1}H NMR spectra (250 MHz) of [Cu(I)(calix[6]PN_3)]OTf in CD_2Cl_2 at 210 K (top), after addition of 30 equiv of EtOH (middle), and subsequent bubbling of CO (bottom). The dots denote the *t*Bu resonances.

spectrometry confirmed that no oxidation of the ligand itself had occurred, giving the complex peak $m/z = 1505.5$ corresponding to $[Cu(I)(calix[6]PN_3)]^+$.

Comparison of the Coordinating Properties of Calix[6]PN_3 and Calix[6]tren-based Cu Complexes. We now address the question of the comparison of a $P^{Ar}N_3$ core with a tren core. The major difference between these two calix-based ligands lies in the nature of the apical donor, which is either a nitrogen atom or a phosphorus atom (of the $P(Ar)_3$ type), the three other donors being essentially identical. The fact that the chelate ring is either 5 or 6 will be tentatively addressed by means of computer modeling of a $N^{Ar}N_3$ core (vide infra).

Cu(I). Stronger Binding to MeCN. The coordination of copper(I) to a tren unit covalently linked to a calix[6]arene core has been previously studied and reported.[34] In this system, it has been shown that the cuprous center displays only a moderate affinity for nitrilo ligands, which stands in contrast to the calix[6]PN_3 analogue. Indeed, [Cu(I)(calix[6]-tren)]$^+$ was shown to bind RCN guests (in a large excess) only at low temperature in dichloromethane, while at RT in pure MeCN, 50% of the calixarene cavities remained empty.

Unusual Affinity for *O*-Donors. Even more surprising is the comparison of the coordinative behavior of the cuprous center vs *O*-donors. With all nitrogen-based calix-ligands we have studied so far, and with tren as a cap in particular, we have never been able to detect any interaction of the Cu(I) center with guest ligands such as an alcohol or an amide. Hence, the NMR study with calix[6]PN_3 highlighted a relatively good affinity for ethanol and DMF that were observed as guest ligands at low *T*. The solution behavior of the "empty cavity" complex $[Cu(I)(calix[6]tren)]^+$ was different as well from the behavior of $[Cu(I)(calix[6]PN_3)]^+$ at low temperature. For the tren derivative, *t*Bu groups underwent self-inclusion into the calix-cavity, which stands in contrast to the $P^{Ar}N_3$ -based complex that remained C_3 symmetrical. This suggests that the calix-cavity was empty in the tren case, whereas in the case of the PN_3 derivative, the cavity was filled with guest molecules not detected by ^{1}H NMR, possibly water.[46]

CO Binding. CO binding to the $[Cu(I)calix[6]PN_3]^+$ complex was characterized by an absorption at $\nu_{CO} = 2085$ cm^{-1}, which lies in between the values measured for the calix[6]tren-based complex (2075 cm^{-1}) and the calix[6]-tris(imidazole) one (2092−2102 cm^{-1}). This shows that the axial nitrogen atom in the tren cap enriches more efficiently the Cu(I) center for π-back bonding to CO than the triphenyphosphine moiety does.

O_2 Interaction. Even more spectacular is the fact that dioxygen had no effect on the $[Cu(I)calix[6]PN_3]^+$ complex, neither in the solid state nor in solution, whereas $[Cu(I)(calix[6]tren)]^+$ displays a very high reactivity, even at low *T*, leading to the oxidation of its Cu(I) center into Cu(II) with either concomitant release of superoxide or oxygen insertion into the ligand, depending on the experimental conditions (non-coordinating solvent such as CH_2Cl_2 vs coordinating solvent such as MeCN).

Cu(II). Geometry. According to the spectroscopic data recorded in solution (EPR and UV−vis), the Cu(II) complexes display structures closer to TBP for calix[6]PN_3 than for calix[6]tren. This is also illustrated by the XRD structures: the τ value[47] is 0.70 for $[Cu(II)(calix[6]tren)(EtOH)]^{2+}$, whereas it is 0.86 for $[Cu(II)(calix[6]PN_3)(DMF)]^{2+}$.

Affinities. Competition experiments gave the following order of relative affinities of Cu(II) for L: EtOH (1) < MeCN (8.6) ≪ DMF (1400). These values are quite different from those found for the analogous tren [MeCN (1) < EtOH (3.7) < DMF (7.1)] and tris-imidazole[48] [MeCN (1) < EtOH (3) < DMF (10)] Cu(II) calix-systems. With the $P^{Ar}N_3$ cap, the affinity of MeCN is surprisingly higher than that of EtOH, and DMF displays an impressively high affinity for the Cu(II) center in comparison to the other complexes.

Such unusual properties for a Cu center embedded in a $P^{Ar}N_3$ core compared to the all-nitrogen tren ligand are quite probably related to the particular electronic structure the P axial soft atom confers to the frontier orbitals of the complexes. For a better understanding, electronic absorption measurements were undertaken together with DFT calculations.

Electronic Structure of the $P^{Ar}N_3$-Based Cu Complexes. Electronic Absorption of the Cu(I) Complexes. The UV−vis spectrum of the $[Cu(I)PN_3(MeCN)]^+$ complex dissolved in distilled MeCN showed a first strong absorption band at 222 ($\varepsilon \sim 12\,600$ M^{-1} cm^{-1}) with a shoulder at 260 nm ($\varepsilon = 2600$ M^{-1} cm^{-1}) assignable to $\pi-\pi^*$ transitions of the phenyl groups, and a third absorption at 318 nm ($\varepsilon = 1600$ M^{-1} cm^{-1}).[49] The UV−vis spectrum of the isolated $[Cu(I)(calix[6]PN_3)]OTf$ complex dissolved in dry CH_2Cl_2 also displayed three absorptions (Figure 6). The first two at 232 nm ($\varepsilon = 38000$ M^{-1} cm^{-1}) and 270 nm ($\varepsilon = 8000$ M^{-1} cm^{-1}) are characteristic of the $\pi-\pi^*$ transitions of the phenyl

(47) Addison, A. W.; Rao, T. N.; Reedijk, J.; van Rijn, J.; Verschoor, G. C. *Dalton Trans.* **1984**, 1349–1356.
(48) Le Clainche, L.; Giorgi, M.; Reinaud, O. *Inorg. Chem.* **2000**, *39*, 3436.
(49) Free ligand in CH_2Cl_2/MeCN 1:1 v/v: λ_{max} (nm) = 230 ($\varepsilon \sim 20000$ M^{-1} cm^{-1}) and 283 ($\varepsilon = 9600$ M^{-1} cm^{-1}).

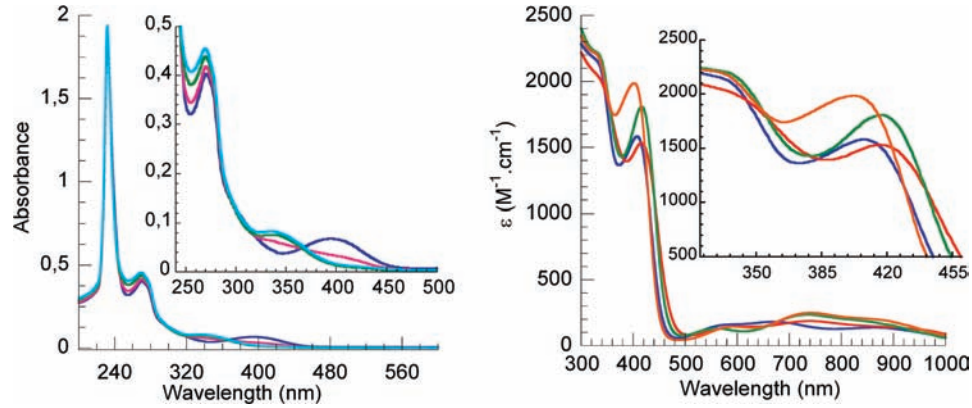

Figure 6. Left: UV−vis spectra of $[Cu(I)(calix[6]PN_3)]^+$ in CH_2Cl_2 (5×10^{-5}M) with progressive addition of MeCN aliquots (in $[Cu(I)(calix[6]PN_3)]OTf$, (0.2, 0.4, 0.6% v/v). Right: UV−vis spectra of $[Cu(II)(calix[6]PN_3)(L)](ClO_4)_2$.[35] Inset: λ_{max}/nm (ε/M^{-1} cm^{-1}), L = H_2O (blue), 408 (1580); EtOH (red), 416 (1530); MeCN (green), 417 (1810); DMF (orange), 402 (1990).

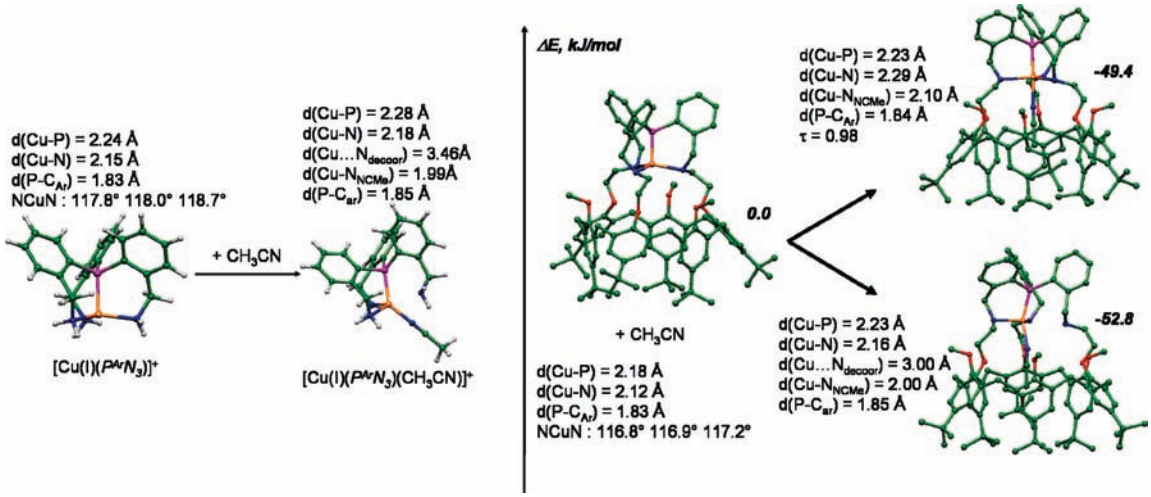

Figure 7. Optimized structures for the small ($[Cu(P^{Ar}N_3)]^+$ and $[Cu(P^{Ar}N_3)(MeCN)]^+$) (left) and the large ($[Cu(calix[6]PN_3)]^+$ and $[Cu(calix[6]PN_3)(MeCN)]^+$) models (right). For the sake of clarity the hydrogen atoms are not represented for the large models.

and phenoxyl moieties of the calixarene capped ligand. A third lower energy absorption band was observed at 395 nm (ε = 1340 M^{-1} cm^{-1}). For both complexes, the lower energy absorptions, which are responsible for the respective light yellow and intense yellow-orange colors of these complexes, were at first sight of unknown origin. When aliquots of MeCN were added to the CH_2Cl_2 solution of the $[Cu(I)(calix[6]PN_3)]OTf$ complex, this third absorption progressively vanished whereas a new one appeared at a higher energy (335 nm, ε = 1540 M^{-1} cm^{-1}). These absorption changes were accompanied by the appearance of an isosbestic point at 365 nm and are thus assignable to the coordination change at the cuprous center because of the binding of MeCN. Indeed, the isolated pale yellow complex $[Cu(calix[6]PN_3)(MeCN)]PF_6$ dissolved in CH_2Cl_2 displayed the same high energy absorptions for the calixarene core at 232 and 270 nm, with two weaker absorptions at 335 and 395 nm, the intensity of which depended on the concentration. Addition of excess MeCN to the solution led, as for the triflate derivative, to the vanishing of the 395 nm band to the benefit of the lowest energy transition at 335 nm.

Electronic Absorption of the Cu(II) Complexes.[35] As displayed in Figure 6 (right), the dicationic Cu(II) complexes based on the calix[6]PN_3 ligand display UV−vis spectra that vary with respect to the guest ligand. The lower energy absorption (500−1000 nm) corresponds to d-d transitions, consistent with a TBP geometry. The high energy absorption (<350 nm) stems from $\pi-\pi^*$ transitions of the ligand. The most interesting and intriguing feature is the relatively strong absorption at about 400 nm that varies only little with the nature of the guest L and that is present even when the guest ligand is not a π donor.

Theoretical Modeling of the Cu(I) Complexes. To get further insights into the structural and electronic properties of these compounds, theoretical calculations (DFT) were undertaken for the non-calixarene complex $[Cu(I)P^{Ar}N_3]^+$ depicted in Figure 7. The optimized structure exhibits a trigonal pyramidal arrangement at the copper center which is slightly out of the basal plane. These geometrical features match closely those derived from the X-ray measurements published by Lang and colleagues for analogous systems.[37] This is, for instance, the case for the Cu(I)−N and Cu(I)−P bond lengths (DFT: 2.147 and 2.239Å, respectively; XRD: 2.171 and 2.185Å, respectively) or for the NCuN and PCuN angles (DFT: 118.2 and 97.0°, respectively; XRD: 118.1 and 98.1° respectively). A supplementary acetonitrile molecule was then introduced to investigate the possible formation of a $[Cu(P^{Ar}N_3)(MeCN)]^+$ adduct. Along the optimization

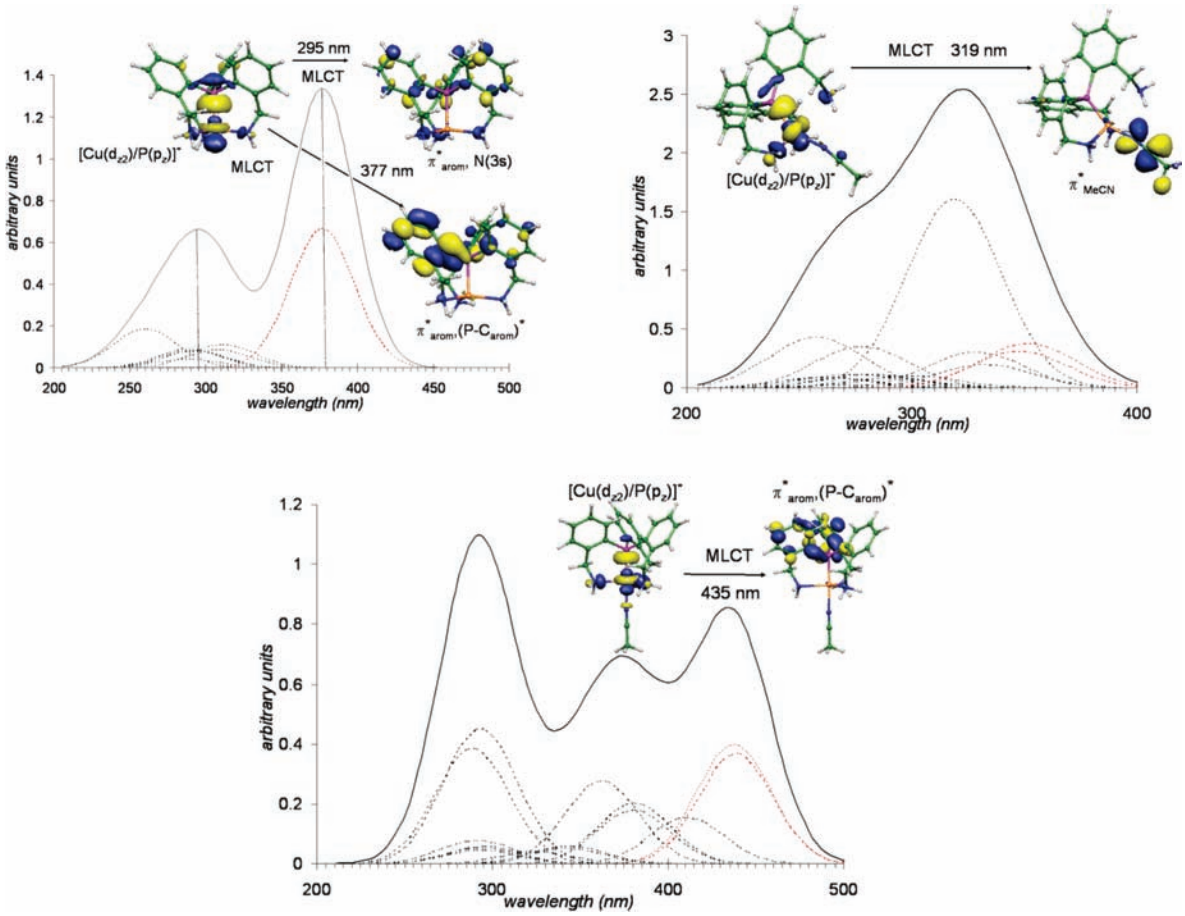

Figure 8. Simulated electronic spectra reporting the main molecular orbitals involved in the most important transitions for $[Cu^{I}(\boldsymbol{P^{Ar}N_3})]^+$ (top, left) and $[Cu^{I}(\boldsymbol{P^{Ar}N_3})(MeCN)]^+$ (top right and bottom). The *y* values are proportional to the oscillator strengths (see the Computational Details section).

process, it appeared that the starting TBP adduct $[Cu(\boldsymbol{P^{Ar}N_3})(MeCN)]^+$ underwent decoordination of one basal nitrogen atom of the $\boldsymbol{P^{Ar}N_3}$ ligand to yield a tetrahedral four-coordinate species. It is worth mentioning that such a geometrical arrangement of a Cu(I)$\boldsymbol{P^{Ar}N_3}$ core has already been characterized by XRD in the case of a nitrate ligand.[37] However, such a conformational rearrangement remains questionable for the $[Cu(calix[6]PN_3)(MeCN)]^+$ complex in view of the possible steric constraints induced by the covalent linkage of the $\boldsymbol{P^{Ar}N_3}$ cap to the calixarene core. Further geometry optimizations were thus undertaken for the *full* $[Cu(calix[6]PN_3)]^+$ and $[Cu(calix[6]PN_3)(MeCN)]^+$ entities to address this point. For the precursor complex (without MeCN), no significant geometrical differences between the small model and the calix-based system have been noticed. The computational strategy of restraining the full ligand to its cryptand part thus seems adequate. On the other hand, the coordination of the acetonitrile molecule on the calix-system revealed that two isomers can be obtained: both of them are associated to a strong binding energy of about −50 kJ/mol. One isomer exhibits a TBP geometry ($\tau = 0.98$) whereas the other one, slightly more stable, exhibits a distorted tetrahedral geometry with decoordination of one basal nitrogen atom of the calix[6]PN_3 ligand (the corresponding N···Cu distance is now 3.00 Å). Even though MeCN is obviously more constrained in the cavity than in the $[Cu(\boldsymbol{P^{Ar}N_3})(MeCN)]^+$ small model, the calixarene appears flexible enough to accommodate a four-coordinate metal center including a MeCN guest.

To get a better understanding of the electronic and structural effects of the complex upon MeCN coordination, the corresponding UV−vis spectra were simulated by means of Time-Dependent DFT (TD-DFT) computations (Figure 8), to be compared with the experimental spectra obtained for $[Cu(calix[6]PN_3)]^+$, with or without acetonitrile (Figure 6). To make the TD-DFT tractable, the previously optimized calix[6]PN_3 complexes were restrained to their cryptand part: the simulated spectra thus take into account the structural constraints imposed by the calixarene.

Let us first qualitatively describe the frontier orbitals that have major contributions in the UV−vis excitations (shown in Figure 8 and SI). The highest occupied molecular orbital (HOMO) of $[Cu(I)\boldsymbol{P^{Ar}N_3}]^+$ results from an anti-bonding interaction between the d_{z^2} copper orbital with the phosphorus lone pair, and will hereafter referred to as: $[Cu(d_{z^2})/P(p_z)]^*$. The lowest unoccupied molecular orbital (LUMO) and LUMO+1 are quasi-degenerated because of symmetry; both display some aromatic π^* character together with a significant $(P-C_{arom})^*$ anti-bonding character. Finally, the LUMO+2 orbital is best described as an aromatic π^* of the triphosphine ligand exhibiting small contributions from nitrogen orbitals. The TD-DFT computations then reveal two main absorption bands for the $[Cu(\boldsymbol{P^{Ar}N_3})]^+$ complex; they are centered at about 295 and 377 nm. Each of them mainly

involves the excitation of one electron from the HOMO toward the aforementioned virtual orbitals. The 295 nm band is mainly due to the HOMO→LUMO+2 transition. The 377 nm band is due to the HOMO→LUMO and HOMO→LUMO+1 transitions, which are almost merged because of quasi degeneracy. It is worth noting that the latter excitations can be considered as a direct influence of the phosphorus atom as both, the LUMO and LUMO+1 orbitals, show a noticeable (P−C_{arom})* anti-bonding character.

As mentioned above, two geometrical arrangements are obtained upon MeCN binding, both of them displaying specific spectral features. For the TBP structure, several weak excitations are found, which lead to three main absorption bands at 292, 375, and 435 nm. The latter is associated to excitations from the HOMO to the π^*_{arom} orbital which exhibits some (P−C_{arom})* character. This transition corresponds to the 377 nm band observed for the precursor complex. The two other bands correspond to excitations from the HOMO toward the π^*_{arom} (about 292 and 360 nm) or to the anti-bonding π^*_{MeCN} orbitals (380 nm).

The four-coordinate complex displays a different spectral signature. An excitation is observed at 350 nm and can be assigned to the transition from the HOMO toward the π^*_{arom} and (P−C_{arom})* orbitals. When compared to the precursor complex, it appears that this excitation has been blue-shifted and is of slightly decreased intensity. The spectrum is largely dominated by a more intense transition at 319 nm which can be associated to an excitation from the HOMO toward a π^*_{MeCN} orbital. Compared to the equivalent excitation within the TBP structure, this transition for the four-coordinate complex appears more intense as testified by the oscillator strengths (0.0857 vs 0.0109).

These values match relatively well the experimental data obtained for the PN_3- and calix[6]PN_3-based complexes. First of all, while the 270 nm $\pi-\pi^*$ transition observed for the calixarene entities may well overlap with the MLCT transition of highest energy, the lower energy transitions can reasonably be attributed to the calculated MLCT band involving the (P−C_{arom})* orbitals, Indeed, the low-energy transition observed experimentally for [Cu(calix[6]PN_3)]$^+$ (395 nm) fits rather well with the calculated transition (377 nm) attributed to the excitation of an electron from the [Cu(d_{z^2})/P(p_z)]* HOMO orbital to the anti-bonding ligand-centered orbital involving a phosphorus (P−C_{arom})* contribution. For the [Cu(calix[6]PN_3)(MeCN)]$^+$ complex, the optimized structures indicate favorable coordination of MeCN in a distorted T_d geometry, a coordination mode which is, however, fully competitive with coordination in a TBP geometry. Interestingly, the TD-DFT computation predicts opposite behaviors of the lowest-energy transition upon coordination of MeCN in one mode or in the other: a 58 nm *red-shift* is expected for the formation of the TBP complex, whereas a 27 nm *blue-shift* is anticipated for the distorted T_d complex. As a matter of fact, the simulated spectrum of the latter species accounts remarkably well for the experimental extinction of the 395 nm band (computed at 377 nm) and for the appearance of a new band at 318 nm (computed at 319 nm) when MeCN is added to the reacting medium.

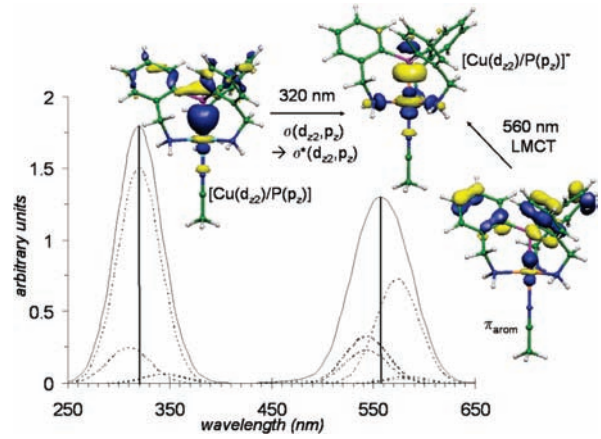

Figure 9. Simulated electronic spectra corresponding to the charge transfer absorptions within the [Cu^{II}(***P^{Ar}N$_3$***)(MeCN)]$^{2+}$ complex. The *y* values are proportional to the oscillator strengths (see the Computational Details section).

The theoretical modeling thus supports the idea of the decoordination of one amino arm and the evolution toward a distorted tetrahedral geometry upon coordination of a guest MeCN.

Theoretical Modeling on *P^{Ar}N$_3$* Cu(II). A similar theoretical study was undertaken on the cupric complex and started with an optimization of the complete [Cu(calix[6]-PN_3)(MeCN)]$^{2+}$ system. The recovered optimized geometry reveals a TBP structure, consistent with the formal +II charge of the metal cation. This structure was then used for TD-DFT UV−vis modeling of the corresponding [Cu(***P^{Ar}N$_3$***)(MeCN)]$^{2+}$ core.

Two charge transfer absorption bands (320 and 560 nm) were obtained (Figure 9). The 320 nm absorption is best described as an excitation from the bonding [Cu(d_{z^2})/P(p_z)] orbital toward the singly occupied molecular orbital (SOMO) which is its anti-bonding counterpart [Cu(d_{z^2})/P(p_z)]*. The 560 nm band corresponds to the excitation from the HOMO-1 toward the SOMO. In the experimental spectrum, only one band is detected. Indeed, the 320 nm band predicted from the calculations is most likely merged into the absorption "wall" arising from the calixarene macrocycle. Therefore, the experimental band observed for complex [Cu-(calix[6]PN_3)(MeCN)]$^{2+}$ at 417 nm can be assigned to the LMCT [π_{arom} → [Cu(d_{z^2})/P(p_z)]*] transition, consistently with the fact that the experimental values measured for various exogenous ligands were found to be very little dependent on the nature of the bound guest (Figure 6). Similar conclusions can be drawn if considering the computations undertaken on a geometrically optimized [Cu(***P^{Ar}N$_3$***)-(MeCN)]$^{2+}$ complex. This indicates that the UV−vis features are dominated by the nature of the ***P^{Ar}N$_3$*** core and that they are only slightly affected by the calixarene cage.

In conclusion, the computed data allow the assignment of the absorption bands at about 300−400 nm for both oxidation states. For the Cu(I) complexes, it is a metal-to-ligand charge-transfer (MLCT) involving the HOMO axial orbital [Cu(d_{z^2})/P(p_z)]* and an empty anti-bonding orbital exhibiting a substantial contribution [π^*_{arom}/(P−C_{arom})*] from the phosphorus atom. The blue shift of this MLCT transition upon

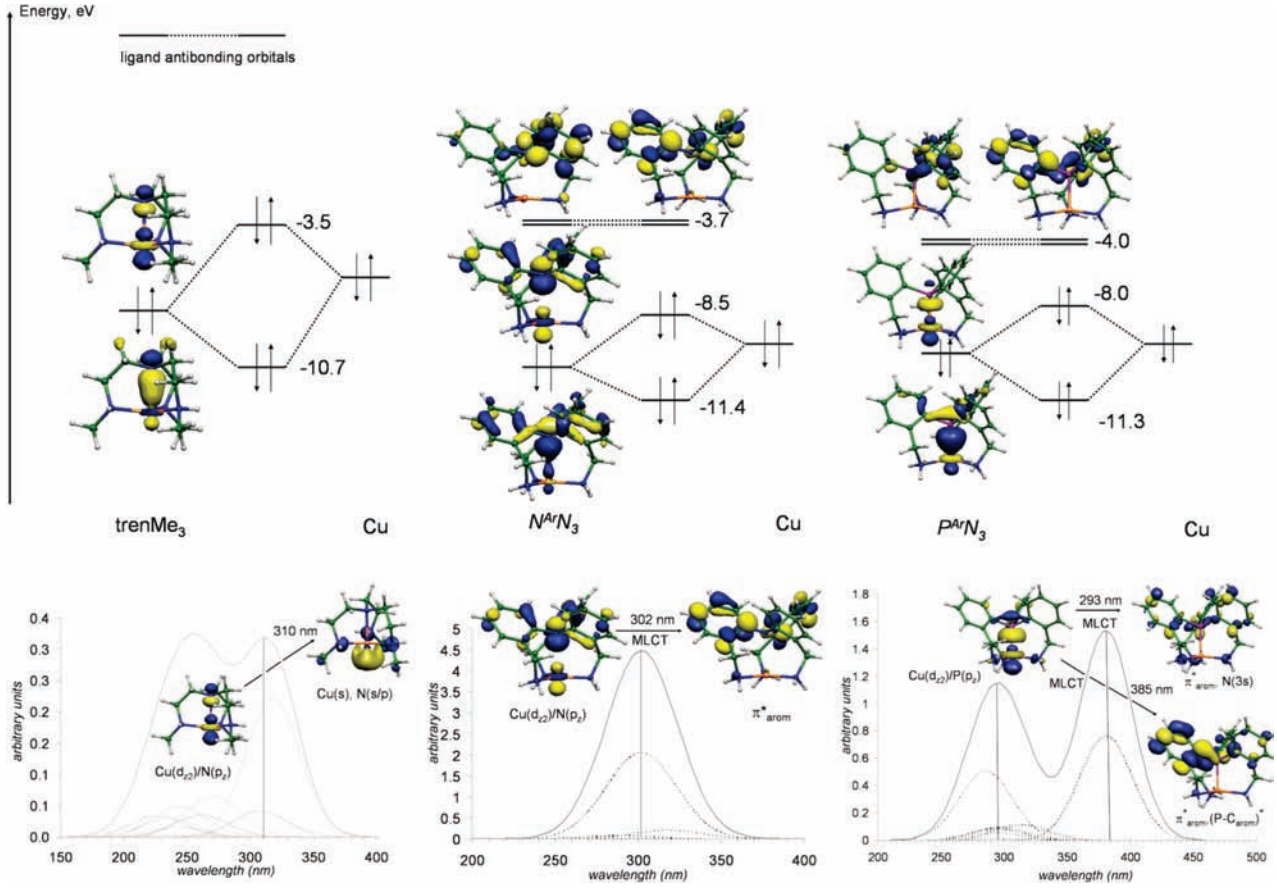

Figure 10. Top: Orbital interactions between the apical atom lone pair and the d_{z^2} copper orbital with the $trenMe_3$ (left), $N^{Ar}N_3$ (middle), and $P^{Ar}N_3$ (right) ligands. For the $trenMe_3$ ligand, it was not possible to clearly identify the anti-bonding orbital involving the apical atom. Bottom: simulated UV−vis spectra of the three complexes. The *y* values are proportional to the oscillator strengths (see the Computational Details section).

MeCN binding to Cu(I) is due to the stabilization of the HOMO orbital. For the Cu(II) state, the absorption at 400−420 nm corresponds to a ligand-to-metal charge transfer (LMCT) $\pi_{arom} \rightarrow [Cu(d_{z^2})/P(p_z)]^*$ band that is barely affected by the guest ligand L. Hence, in both cases, these CT transitions can be related to the P−Cu bond.

Comparison with All-Nitrogen Donors. To highlight the impact of the $P^{Ar}N_3$ ligand, we performed UV−vis computations and analyses on the $[Cu(trenMe_3)]^+$, $[Cu(N^{Ar}N_3)]^+$, and $[Cu(P^{Ar}N_3)]^+$complexes. Each of them has been previously fully optimized. Together, they provide insights into the influence of the chemical nature of the apical ligand (P vs N) and of the nature of the supporting ligand ($X^{Ar}N_3$ vs tren). For these model complexes, the MO diagrams remain qualitatively identical, only the relative energy levels of the orbitals are changed (Figure 10). For the $[Cu(I)trenMe_3]^+$ complex, a MLCT transition is predicted at 310 nm. It is the analogous transition to the 293 nm one computed for the $[Cu(P^{Ar}N_3)]^+$ complex (i.e., the high energy MLCT), and is described as a transition from the $[Cu(d_{z^2})/N(p_z)]^*$ HOMO to a mixture of the vacant orbitals of the equatorial nitrogen (4s/p) and the copper (5s) (LUMO). No transition comparable to that observed at 395 nm is predicted for the $trenMe_3$ model complex. This seems rather logical as it was associated to an excitation toward an aromatic π^* orbital mixed with a significant $P-C_{arom}$ anti-bonding character $[\pi^*_{arom}/(P-C_{arom})^*]$. Indeed, the analogous anti-bonding $[(N_{ap}-C_{tren})^*]$ orbitals are very high in energy in $[Cu(trenMe_3)]^+$ and are not involved in any UV−vis transition. Such a difference between both complexes is not surprising in view of the non-aromatic character of the $trenMe_3$ ligand. The theoretical spectrum of the $[Cu(N^{Ar}N_3)]^+$ complex, which bears three aromatic units, as does $P^{Ar}N_3$, shows a transition toward the $[\pi^*_{aro}/(N_{ap}-C_{aro})^*]$ orbital at about 300 nm, a much higher transition energy than for the $[Cu(P^{Ar}N_3)]^+$ complex (385 nm). We thus conclude that the 395 nm band of $[Cu(P^{Ar}N_3)]^+$ results from a conjugated effect of both, the chemical nature of the apical ligand (*P* vs *N*) and the aromatic character of the ligand (tren vs XN_3). The comparison of the simplified orbital diagrams represented in Figure 10 summarizes these facts for Cu(I) complexes.

The main difference between the $trenMe_3$ complex and the aromatic ($N^{Ar}N_3$ and $P^{Ar}N_3$) species relies in the energetic proximity of a virtual orbital having the same symmetry as the HOMO for the latter. This close vicinity is more pronounced for the $[Cu(P^{Ar}N_3)]^+$ complex ($\Delta E = 4.0$ eV) than for the $[Cu(N^{Ar}N_3)]^+$ complex ($\Delta E = 4.8$ eV). This can be rationalized by considering two points. First, the $Cu-X_{ap}$ length (Cu−P: 2.147 Å vs Cu−N: 2.655 Å, respectively) argues in favor of a stronger metal/apical atom interaction in the $[Cu(P^{Ar}N_3)]^+$ complex, and thus to a higher energy for the anti-bonding $[Cu(d_{z^2})/P(p_z)]^*$ orbital. Second, this interaction should also be exalted by the fact that the phosphorus atom interacts with copper through its 3p orbitals

that are higher in energy than the nitrogen 2p orbitals.[8] They consequently are closer to Cu(d_{z^2}), which implies a larger gap between the bonding and the anti-bonding orbitals resulting from the interaction between the metal and the ligand. These two considerations explain why the HOMO is higher in the $[Cu(\boldsymbol{P^{Ar}N_3})]^+$ complex than in the $[Cu(\boldsymbol{N^{Ar}N_3})]^+$ complex.

The proximity of accepting virtual orbitals having the same symmetry as the HOMO confers original coordination properties to $[Cu(calix[6]PN_3)]^+$. In the cuprous state, these orbitals allow stabilizing the coordination of exogenous hard σ-donor ligands such as alcohols. This is possible because such guests can interact with the d_{z^2} orbital. This stabilizing behavior is lacking in $[Cu(Calixtren)]^+$ because of the high energy of the anti-bonding $(N_{ap}-C_{tren})^*$ orbitals.

On the other hand, in the cupric state, the LMCT $\{\pi_{arom} \rightarrow [Cu(d_{z^2})/P(p_z)]^*\}$ shows an enrichment of the Cu(II) center that is absent in the *tren* system. Consequently, the cupric complex presents an unusually high affinity for a relatively weak σ-donor such as MeCN that binds more strongly than EtOH in the $\boldsymbol{P^{Ar}N_3}$ environment. This stands in contrast to the all-nitrogenous (tren) or N_3O cores provided by the tris(imidazole)-based calixarene ligand.[27] Also, DMF, because of its high dipolar moment, becomes the "winner" ligand by 3 orders of magnitude for $K_{L'/L}$ compared to EtOH,[45] whereas in the tren[31] or tris(imidazole)[27] systems, it is better bound by only a factor of 2 to 3.

Finally, comparison of the molecular diagrams shows a HOMO of higher energy for the tren ligand, which denotes a more electron rich metal center. The energy splitting upon the combination of the Cu d_{z^2} orbital with the ligand orbitals also indicates a stronger interaction between the metal center and tren compared to $\boldsymbol{P^{Ar}N_3}$. These observations account well for the experimentally observed stronger π-back-donation from trenCu(I) to CO, as well as for its much higher reactivity toward O_2. This stands in contrast to the computed model obtained for a PN_3 core that lacks the π system brought by the phenyl substituents.[8] With an alkylphosphine, the σ-donation to Cu(I) was shown to be stronger than for an alkylamine, and opposite conclusions were obtained for the comparative binding of Cu(I) to CO and O_2 with tren. This highlights the importance of the π-accepting system that is present with an axially coordinated $P(Ar)_3$ moiety but lacking with an alkylphosphine as the d orbitals of the phosphorus donor are far too high in energy to play this role.

Conclusion

Comparative experimental analyses of PN_3- and tren-based copper complexes were precluded by the uncontrolled coordination behavior of $PN_3Cu(I)/Cu(II)$ complexes. When covalently linked to the calixarene cone, the $\boldsymbol{P^{Ar}N_3}$ cap is constrained in such a geometry that it can act exclusively as a tripodal cofacial ligand. This allows the stabilization of copper ions in both oxidation states in the coordination core provided by a single $\boldsymbol{P^{Ar}N_3}$ unit. Our studies have shown that the phosphorus donor remains bound to Cu(I), as well as to Cu(II). This made possible, for the first time, a solution study of the properties of a Cu(II) ion bound to a P atom, in spite of the misfit of their HSAB character (relatively hard and soft, respectively). Here, we have presented a complete survey for both Cu(I) and Cu(II) states. In solution, the calixarene complexes readily interact with exogenous guest ligands and surprising coordination properties of the resulting complexes have been highlighted as follows: (i) an unusually high affinity of Cu(I) for σ-donors as hard as an alcohol, (ii) in contrast, an unusually high affinity of Cu(II) for relatively weak σ-donors such as a nitrile, and (iii) a surprising inertness of the $[Cu(calix[6]PN_3)]^+$ complexes toward O_2 that contrasts with the high reactivity of its tren analogue.

Spectroscopic data, together with DFT calculations, have allowed a comparison with nitrogen cores lacking the *P*-donor, thus highlighting the impact the latter has on the electronic properties of the complexes facing various guest donors. In general, we conclude that the $P(Ar)_3$ center tunes the metal ion properties, by absorbing excess electronic density from rich Cu(I) or by injecting electronic density into electron-poor Cu(II). It is indeed the simultaneous presence of both, an apical phosphorus atom and an aromatic supporting ligand, that allows such unusual coordinating behavior of the $[Cu(calix[6]PN_3)]^+$ complex.

Although we cannot extrapolate such properties to the DβH and PHM Cu_M site, this study has highlighted the important impact a soft donor with accepting capacities can have on the copper properties. Interestingly, it seems to tune the metal center properties in opposite directions for Cu(I) and Cu(II): the soft reduced state, Cu(I), better accepts hard donors, whereas the harder oxidized state, Cu(II), better accepts weak donors. As far as O_2 activation is concerned, such modulation of the electronic properties may well have a role as the catalytic cycle involves O_2 binding to Cu(I) to provide a $Cu(II)(O_2^{-\cdot})$ intermediate.

We are now investigating, by electrochemical means, the redox behavior of the $Cu(calix[6]PN_3)$ complexes to get a detailed thermodynamic and kinetic picture on coupled ligand exchange and electron transfer processes.

Experimental Section

General. All solvents and reagents were obtained commercially. All solvents used have been distilled and kept under N_2 or argon. IR spectra were recorded with a Perkin-Elmer Spectrum One spectrometer. EPR spectra were recorded using a Bruker Elexys spectrometer (X-band). Fitting of the EPR spectra was performed using Xepr & Xsophe suite (Bruker). The vis-NIR spectra were recorded with a Jasco V-570 spectrophotometer. Elemental analysis was performed at the Institut des Substances Naturelles, Gif sur Yvette, France.

Safety Note. ***Caution!*** *Although we have not encountered any problems, it is noted that perchlorate salts of metal complexes with organic ligands are potentially explosive and should be handled only in small quantities with appropriate precautions.*

Synthetic Procedures. The ligand $calix[6]PN_3$[50] and its Cu(II) complexes[35] were prepared as previously described. *Tris*(2-carboxaldehyde)triphenylphosphine was synthesized according to the procedure described by Whitnall et al.[39]

(50) Zeng, X.; Hucher, N.; Reinaud, O.; Jabin, I. *J. Org. Chem.* **2004**, *69*, 6886–6889.

***Tris*(2-isopropylimino)triphenylphosphine.** *Tris*(2-carboxaldehyde)triphenylphosphine (300 mg, 0.86 mmol) was dissolved in 20 mL of distilled CH_2Cl_2 in the presence of Na_2SO_4. Isopropylamine was added as a liquid (0.29 mL, 3.57 mmol, 3 equiv) under argon. The reaction mixture was stirred at RT for 18 h, filtered over Celite, and condensed to dryness giving a yellow oily semicrystalline product. After washing with pentane (15 mL) at −78 °C, the yellow crystals were filtered off and air-dried, giving 256 mg (64%) of *tris*(2-isopropylimino)triphenylphosphine. The compound was not further purified but directly engaged in the following reduction step.

^{1}H NMR (250 MHz, $CDCl_3$): δ 1.04 (d, $J = 7$ Hz, 18H, $(Me)_2$), 3.37 (m, $J = 7$ Hz 3H, C*H*$(Me)_2$), 6.84 (dd, $J_{PH} = 5$ Hz, $J_{HH} = 7$ Hz, 3H, ArH *ortho*-P), 7.22 (t, $J = 7$ Hz, 3H, ArH *meta*-P), 7.37 (t, $J = 7$ Hz, 3H, ArH *par*-P), 7.94 (dd, $J_1 = 4$ Hz, $J_2 = 7$ Hz, 3H, ArH *ortho*-CH_2), 8.83 (d, $J = 5$ Hz, 6H, NC*H*$_2$Ar). ^{31}P {H} NMR (101 MHz, $CDCl_3$): δ −28. IR (KBr) ν (cm^{-1}): 3054, 2966, 2924, 2863, 2838, 1943, 1642, 1628, 1459, 1381, 1141, 1116, 883, 760, 551.

***Tris*(2-isopropylamino)triphenylphosphine (Ligand PN_3).** *Tris*(2-isopropylimino)-triphenylphosphine (256 mg, 0.55 mmol) was dissolved in 10 mL of freshly distilled THF, and $LiAlH_4$ (200 mg, 5.5 mmol, 10 equiv) was added under argon. After 17 h of stirring at RT the reaction mixture was cooled down to 0 °C, and 10 mL of NaOH (10%) was added dropwise. The mixture was filtered over Celite, the aqueous phase separated and extracted twice with CH_2Cl_2 (10 mL). The organic phases were assembled, washed with water, dried over Na_2SO_4, and condensed to dryness. The resulting yellow oil was finally triturated with ether giving 248 mg (96%) of pure *tris*(2-isopropylamino)triphenylphosphine as a sticky solid.

^{1}H NMR (250 MHz, $CDCl_3$): δ 0.87 (d, $J = 7$ Hz, 18H, $(Me)_2$), 2.62 (m, $J = 7$ Hz 3H, C*H*$(Me)_2$), 3.94 (s, 6H, CH_2), 6.83 (dd, $J_{PH} = 4$ Hz, $J_{HH} = 7$ Hz, 3H, ArH *ortho*-P), 7.15 (t, $J = 7$ Hz, 3H, ArH *meta*-P), 7.33 (t, $J = 7$ Hz, 3H, ArH *para*-P), 7.44 (dd, $J_1 = 4$ Hz, $J_2 = 7$ Hz, 3H, ArH *ortho*-CH_2). ^{31}P {H} NMR (101 MHz, $CDCl_3$): δ −37. IR (CH_2Cl_2) ν (cm^{-1}): 3315, 3061, 2966, 2930, 2870, 1466, 1439, 1380, 1337, 1173, 1120, 1059. UV−vis. (CH_2Cl_2/MeCN) λ_{max} (nm) = 235 ($\varepsilon \sim 20000$ M^{-1} cm^{-1}), 283 nm ($\varepsilon = 9600$ M^{-1} cm^{-1}). MS (ES) (CH_2Cl_2) *m*/*z* 476.3177 (100) (calcd. for $[M+H^+]$: 476.3195).

$[Cu(II)PN_3](ClO_4)_2$. A solution of PN_3 (20 mg, 0.042 mmol) in 250 μL of distilled CH_2Cl_2 was added under argon to $[Cu(H_2O)_6](ClO_4)_2$ (15.4 mg, 0.042 mmol) in 250 μL of distilled CH_3CN. The reaction mixture turned green immediately and was stirred at RT for 1 h. The solvent was evaporated, and the resulting green solid was washed twice with CH_2Cl_2 giving 9.6 mg (55%) of green solid.

EPR (solid state, X-band, 100 K): $g_1 = 2.010$ ($A_1^P = 195$, $A_1^{Cu} = 27 \times 10^{-4}$ cm^{-1}); $g_2 = 2.050$ ($A_1^P = 228$, $A_1^{Cu} = 30.10^{-4}$ cm^{-1}); $g_3 = 2.220$ ($A_1^P = 20$, $A_1^{Cu} = 172.10^{-4}$ cm^{-1}). IR (solid) ν (cm^{-1}): 3268, 3063, 2975, 2869, 1467, 1140, 1399, 1387, 1206, 1097, 760 (ClO_4).

$[Cu(I)(PN_3)]PF_6$. A solution of PN_3 (35.5 mg, 0.075 mmol) in 500 μL distilled and deoxygenated CH_2Cl_2 was added under argon to $[Cu(CH_3CN)_4]PF_6$ (27.8 mg, 0.075 mmol) in 500 μL of distilled and deoxygenated CH_3CN. The resulting pale yellow solution was stirred at RT for 1 h. The solvent was evaporated, and the pale yellow solid was washed twice with Et_2O giving 51.2 mg (94%) of complex $[Cu(I)(PN_3)]PF_6$.

^{1}H NMR (250 MHz, CD_3CN): δ 1.02 (d, $J = 6$ Hz, 18H, $(Me)_2$), 2.88 (quin, $J = 6$ Hz, 3H, C*H*$(Me)_2$), 6.82 (t, $J = 7$ Hz, 3H, ArH *ortho*-P), 7.25 (t, $J = 7$ Hz, 3H, ArH *meta*-P), 7.45 (t, $J = 7$ Hz, 3H, ArH *para*-P), 7.52 (dd, $J_1 = 4$ Hz, $J_2 = 7$ Hz, 3H, ArH *ortho*-CH_2). ^{31}P {H} NMR (101 MHz, CD_3CN): δ −37 (broad s, fwhh = 1515 Hz, $[Cu(PN_3)]^+$), −62.5 (sept, $J = 710$ Hz, PF_6,). IR (CH_2Cl_2) ν (cm^{-1}): 3276, 3070, 2971, 2873, 1466, 1442, 1387, 1341, 1204, 1155, 1124, 1031. UV−vis. (MeCN) λ_{max} (nm) = 222 ($\varepsilon \sim 12\ 600$ M^{-1} cm^{-1}), 260 nm (sh) ($\varepsilon = 2600$ M^{-1} cm^{-1}, 318 nm ($\varepsilon = 1600$ M^{-1} cm^{-1}). MS (ES) (CH_3CN) *m*/*z* 538.2406 (100) (calcd for $[M]^+$: 538.2412).

$[Cu(I)(calix[6]PN_3)]OTf$. To a mixture of calix[6]PN_3 (51 mg, 0.036 mmol) and $[Cu(OTf)](tol)_{1/2}$ (9.32 mg, 0.036 mmol) was added 4.5 mL of deoxygenated toluene under argon. The resulting yellow-orange colored solution was stirred for 2 h at RT. The solvent was evaporated and the resulting bright yellow solid was washed twice with pentane giving 56.3 mg (94%) of complex $[Cu(I)(calix[6]PN_3)]OTf$.

^{1}H NMR (250 MHz, CD_2Cl_2): δ 0.78 (s, 27H, *t*Bu), 1.39 (s, 27H, *t*Bu), 3.07 (broad s, 6H, NCH_2), 3.47 (d, $J = 15$ Hz, 6H, $ArCH_2$ (eq)), 3.65 (broad s, 3H, NH), 3.75 (s, 9H, OCH_3), 4.02 (broad s, -H, NCH_2Ar), 4.29 (s, 6H, OCH_2), 4.44 (d, $J = 15$ Hz, 6H, $ArCH_2$ (ax)), 6.63 (s, 6H, ArH), 6.82 (broad s, 3H, PArH), 7.33 (s, 6H, ArH), 7.40 (m, 3H, PArH), 7.47 (m, 6H, PArH). ^{31}P {H} NMR (201 MHz, CD_2Cl_2): δ −70 (s, fwhh = 793 Hz). MS (ES) (CH_2Cl_2) *m*/*z* 1504.8240 (100) (calcd. for $[M]^+$: 1504.8211).

$[Cu(calix[6]PN_3)(MeCN)]PF_6$. A solution of calix[6]$PN_3$ (28.9 mg, 0.020 mmol) in 2 mL of doxygenated CH_2Cl_2 was added under argon to a solution of $[Cu(CH_3CN)_4]PF_6$ (7.5 mg, 0.020 mmol) in 1 mL of doxygenated CH_3CN. The resulting pale yellow solution was stirred for 30 min at RT, and the solvent was then evaporated giving complex $[Cu(I)(calix[6]PN_3)(CH_3CN)]PF_6$ as a pale yellow solid.

^{1}H NMR (250 MHz, CD_2Cl_2): δ −1.15 (broad s, $MeCN_{in}$), 0.76 (s, 27H, *t*Bu), 1.40 (s, 27H, *t*Bu), 2.95 (broad s, 6H, NCH_2), 3.48 (d, $J = 15$ Hz, 6H, $ArCH_2$ (eq)), 4.01 (s, 9H, OCH_3), 4.12 (broad s, 6H, OCH_2), 4.48 (d, $J = 15$ Hz, 6H, $ArCH_2$ (ax)), 6.57 (s, 6H, ArH), 7.00 (broad s, 3H, PArH), 7.33 (m, 6H, ArH), 7.33 (m, 3H, PArH), 7.51 (broad s, 6H, PArH). ^{31}P {H} NMR (101 MHz, CD_2Cl_2): δ −46 (s, fwhh = 304 Hz), 61.3 (sept, $J = 710$ Hz, PF_6,). IR (CH_2Cl_2) ν (cm^{-1}): 2964, 2906, 2869, 1481, 1363, 1298, 1199, 1120, 1011. MS (ES) (CH_3CN) *m*/*z* 1504.8211 (100) (calcd. for $[M\text{-}CH_3CN]^+$: 1504.8211).

Computational Details

Except for the geometry optimizations performed on the large models, all calculations were carried out with the GAUSSIAN03 suite of programs[51] within the DFT approach. The B3LYP functional was used, together with the DZVP2 basis set[52] augmented by a set of p diffuse orbitals on nitrogen and phosphorus atoms[53] in line with our previous works.[8,10,54,55] For the geometry optimization of the large models, the DFT deMon2k[56] code was used with the GEN-A2 auxiliary function set. Because of the unavailability of the B3LYP functional in deMon, the PBE functional was used.[56] Following the geometry optimization of the ground states, the first

(51) Frisch, M. J. et al. *Gaussian 03*, Revision A.1; Gaussian, Inc.: Pittsburgh, PA, 2003.
(52) Godbout, N.; Salahub, D. R.; Andzelm, J.; Wimmer, E. *Can. J. Chem.* **1992**, *70*, 560–571.
(53) Clark, T.; Chandrasekhar, J.; Schleyer, P.; Ragué, V. *J. Comput. Chem.* **1983**, *4*, 294–301.
(54) de la Lande, A.; Moliner, V.; Parisel, O. *J. Chem. Phys.* **2007**, *126*, 035102.
(55) de la Lande, A.; Gérard, H.; Parisel, O. *Int. J. Quantum Chem.* **2008**, *108*, 1898–1904.
(56) Köster, A. M.; Calaminici, P.; Casida, M. E.; Flores-Moreno, R.; Geudtner, G.; Goursot, A.; Heine, T.; Ipatov, A.; Janetzko, F.; del Campo, J. M.; Patchkovskii, S.; Ulises Reveles, J.; Salahub, D. R.; Vela, A. (deMon developers) 2006.

excited states were calculated within the TD-DFT framework,[57] a procedure now widely used to deal with electronic spectra[58] and which has already been applied to Cu or Zn organometallic species.[59] To facilitate comparison between the experimental and the theoretical data, the UV−vis spectra were simulated. Every single absorption band has been represented by a Gaussian function $G(\lambda)$ centered at the absorption wavelength λ_{exc}; the height of them are proportional to the corresponding oscillator strength scaled by a factor 1000 (OS) (dotted lines on Figures 8, 9, and 10). The Full Width at Half Maximum (FWHM), related to the standard deviation σ, was set to 50 nm,[60] and the following formulation was retained for each individual transition:

$$G(\lambda) = \frac{1}{\sigma\sqrt{2\pi}} OS \exp\left[\frac{-(\lambda - \lambda_{exc})^2}{2\sigma^2}\right]$$

$$FWHM = 2\sqrt{2 \ln 2}\sigma$$

The summation of all Gaussian functions was then operated to obtain the final simulated spectra (full line in the simulated spectra reported).

Acknowledgment. This work was supported by CNRS, Ministère de la Recherche and Agence National pour la Recherche (Calixzyme Project ANR-05-BLAN-0003). The calculations have been performed at IDRIS (F. 91403, Orsay, France) and CINES (F. 34000 Montpellier, France) national supercomputing centers, as well as at the CCRE of the University Paris 6 (F. 75252, Paris, France).

Supporting Information Available: Comparative ^{1}H and ^{31}P NMR δ shifts for ligands and complexes displayed as tables, partial molecular orbital diagrams calculated for $\boldsymbol{P^{Ar}N_3}$-based Cu complexes. This material is available free of charge via the Internet at http://pubs.acs.org.

IC802253T

(57) Burke, K.; Gross, E. K. U. A Guided Tour of Time-Dependent Density Functional Theory. In *Density Functionals: Theory and Applications*; Springer: Berlin, 1998; p 117.
(58) See (and references therein), for some recent instances: Ciofini, I.; Daul, C. A.; Adamo, C. *J. Phys. Chem. A* **2003**, *107*, 11182–11190. (b) Gutierrez, F.; Rabbe, C.; Poteau, R.; Daudey, J.-P. *J. Phys. Chem. A* **2005**, *109*, 4325–4330. (c) Cornard, J.-P.; Lapouge, C. *Chem. Phys. Lett.* **2007**, *438*, 41–46.
(59) See, for instance: (a) Clark, A. E.; Davidson, E. R.; Zaleski, J. M. *Chem. Commun.* **2003**, 2876–2877.
(60) Cavillot, V.; Champagne, B. *Chem. Phys. Lett.* **2002**, *354*, 449–457.